Coupled-channel meson electroproduction analysis

Michael Doering

With J. Hergenrather, M. Mai, T. Mart, U.-G. Meissner, D. Roenchen,

Y.-F. Wang, R. Workman









Department of Energy, DOE DE-AC05-06OR23177 & DE-SC0016582



HPC support by JSC grant jikp07



National Science Foundation Grant No. PHY 2012289

Degrees of freedom: Quarks or hadrons

Resonance review [Mai 2022]



QCD at low energies

Non-perturbative dynamics

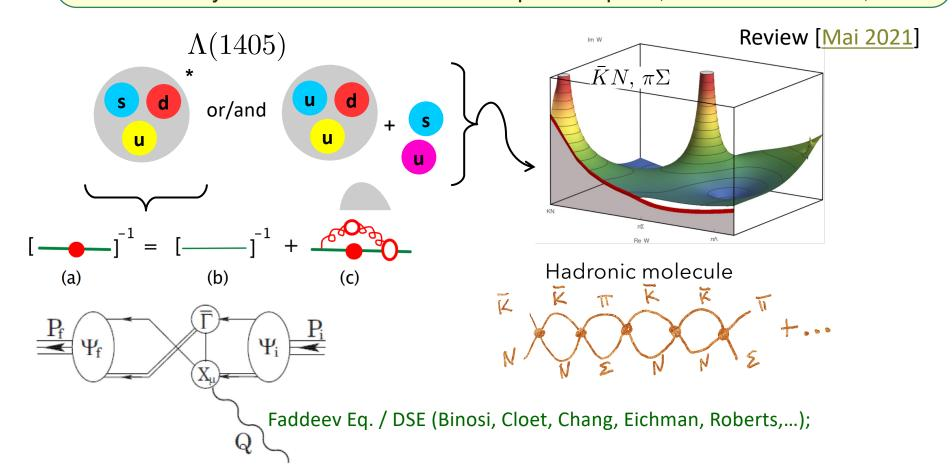
→ rich spectrum of excited states

How many states are there?

→ missing resonance problem (does it exist?)

What are they?

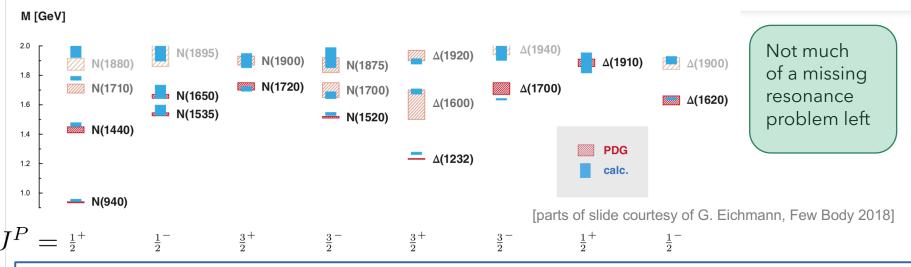
→ 2-quark/3-quark, hadron molecules, ...

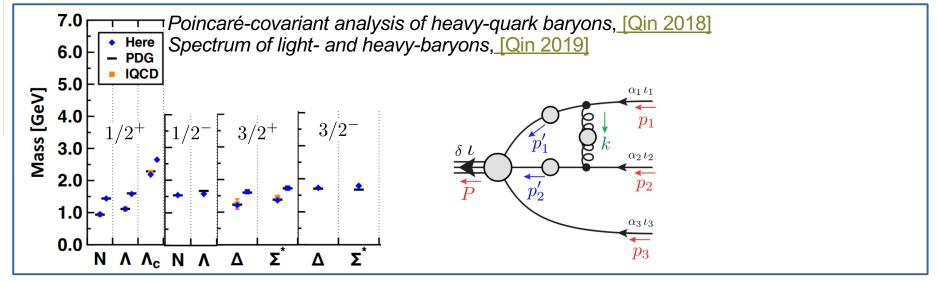




Light baryons from diquark dynamics

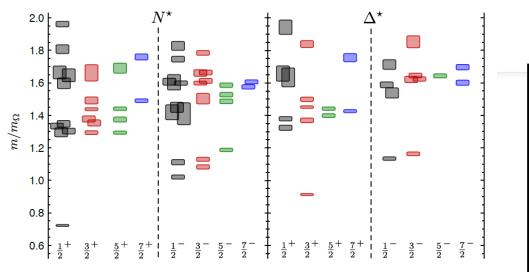
Quark-diquark with reduced pseudoscalar + vector diquarks: [Eichmann (2016]





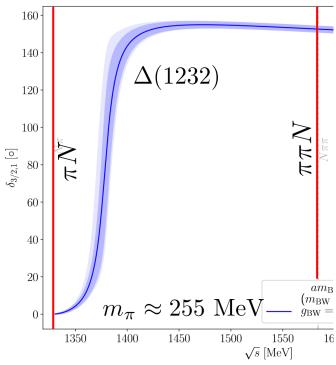


Lattice QCD for excited baryons



 $m_{\pi} = 396 \,\mathrm{MeV} \,[\mathrm{Edwards}\,et\,al.,\,\mathrm{Phys.Rev.}\,\mathrm{D84}\,(2011)]$

- Information on existence, width & properties of resonances requires
 - Meson-baryon interpolating operators
 - Detailed finite-volume analysis



[G. Silvi et. al., <u>arXiv: 2101.00689</u>] See also: Bulava et al., [<u>2208.03867</u>]

How about $\pi\pi N$? 3B Dynamics?

Phenomenology of the baryon spectrum

Review by [Thiel, Afzal, Wunderlich 2022]



Dynamical coupled-channel approaches

[MD, M. Mai, J. Haidenbauer, T. Sato, upcoming review]

- ANL-Osaka (former: EBAC) [Kamano et al.]
- Dubna-Mainz-Taipei model [<u>Tiator</u>]
- Jülich-Bonn(-Washington) [Rönchen]
- . . .
- Characteristics:
 - Direct fit to data (pion & photon-induced)
 - Simultaneous fit to data of different final states
 - Integral scattering equation as needed for proper treatment of three-body channels ($\pi\pi N$) & inclusion of lefthand cut

Note: Only a subclass of analysis efforts; see, e.g., Bonn-Gatchina group K-matrix approach



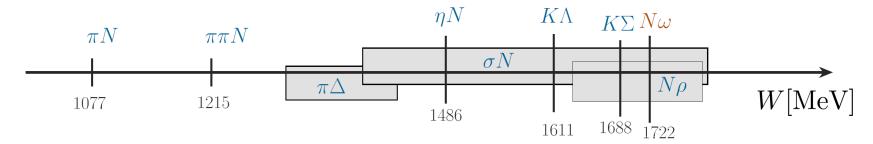
JBW DCC approach (Jülich-Bonn-Washington)

The scattering equation in partial-wave basis

$$\langle L'S'p'|T_{\mu\nu}^{IJ}|LSp\rangle = \langle L'S'p'|V_{\mu\nu}^{IJ}|LSp\rangle +$$

$$\sum_{\gamma,L''S''}\int_{0}^{\infty}dq \quad q^{2} \quad \langle L'S'p'|V_{\mu\gamma}^{IJ}|L''S''q\rangle \frac{1}{E-E_{\gamma}(q)+i\epsilon} \langle L''S''q|T_{\gamma\nu}^{IJ}|LSp\rangle$$

• channels ν , μ , γ :



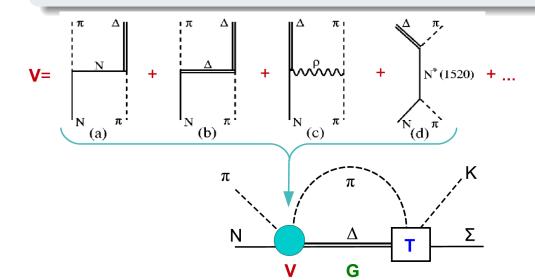


JBW DCC approach (Jülich-Bonn-Washington)

The scattering equation in partial-wave basis

$$\langle L'S'p'|T^{IJ}_{\mu\nu}|LSp\rangle = \langle L'S'p'|V^{IJ}_{\mu\nu}|LSp\rangle +$$

$$\sum_{\gamma,L''S''} \int_{0}^{\infty} dq \quad q^{2} \quad \langle L'S'p'|V^{IJ}_{\mu\gamma}|L''S''q\rangle \frac{1}{E - E_{\gamma}(q) + i\epsilon} \langle L''S''q|T^{IJ}_{\gamma\nu}|LSp\rangle$$



- potentials V constructed from effective \mathcal{L}
- s-channel diagrams: T^Pgenuine resonance states
- t- and u-channel: T^{NP}
 dynamical generation of poles
 partial waves strongly correlated
- contact terms



Transitions in s, t, and u-channels

- 21 s-channel exchanges (resonance)
- Contact terms
- t and u-channel exchanges:

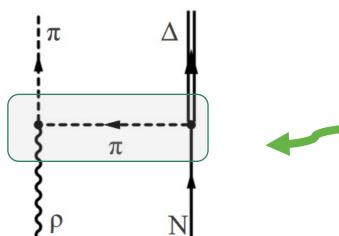
[Yu-Fei Wang 2022]

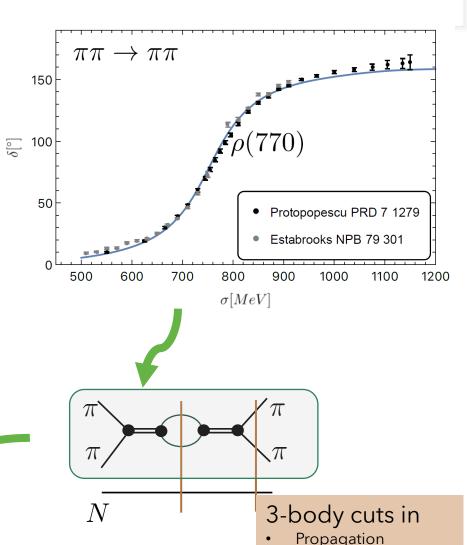
μ	πN	ηN	$K\Lambda$	$K\Sigma$	ωN	$\pi\Delta$	σN	ho N
πN	$(\pi\pi)_{\sigma}, \ (\pi\pi)_{ ho}, \ N, \Delta$	a_0,N	K^*, Σ, Σ^*	$K^*, \Lambda, \Sigma, \Sigma^*$	ho,N	$ ho,N,\Delta$	π,N	$\pi,\omega,\ a_1,N,\ \Delta,C$
ηN		N,f_0	K^*, Λ	K^*, Σ, Σ^*	ω,N			
$K\Lambda$			$\omega, f_0, \phi, \Xi, \Xi^*$	$ \rho, a_0, \\ \Xi, \Xi^* $	$K,K^*,\ \Lambda$			
$K\Sigma$				$ ho,\omega,\phi,\ f_0,a_0,\ \Xi,\Xi^*$	$K, K^*, \ \Sigma, \Sigma^*$			
ωN		7			σ, N			
$\pi\Delta$		\		π		$ ho,N,\Delta$	π	π,N
σN		ИХ	π	π			σ, N	
ho N	$t (N\overline{N} \rightarrow \tau)$	ππ) \	σ, ρ	π				$ ho,N,\ \Delta,C$
		IN/I	$S (\pi N \rightarrow \pi N)$	π				



Three-body channels $\sigma N, \pi \Delta, \rho N$

- Resonant sub-channels
- Fit 2→2 amplitude to 2→ 2
 scattering data
- Include as sub-channel in 3-body amplitude:
- 3-body unitarity: Requires, e.g.



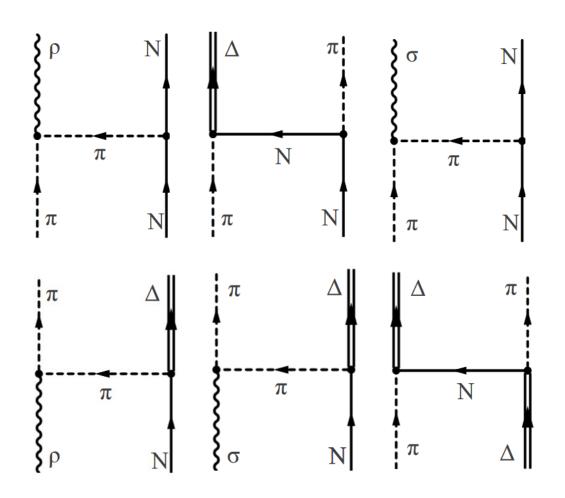


exchange



$2 \rightarrow 3$ and $3 \rightarrow 3$ body unitarity

• Unitarity requires certain transition amplitudes



 $2\rightarrow3$

Unitarity requires formulation of scattering via integral equation
→ ANL-Osaka & JB(W)

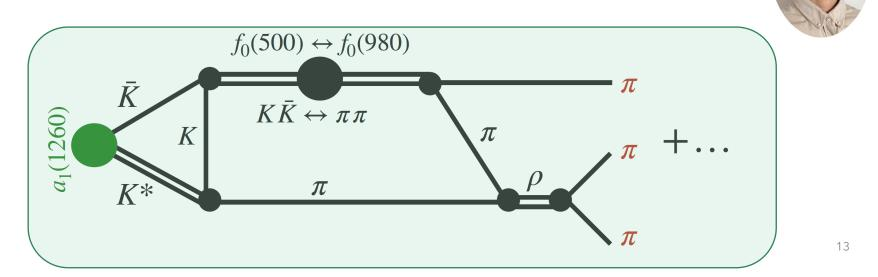
3**→**3



Unitary amplitudes for meson analysis

[Y. Feng, F. Gil, R. Molina, M. Mai, V. Shastry, A. Szczepaniak, et al.]

Talk tomorrow morning







JB: Data base

• $\pi N \rightarrow X$: > 7,000 data points ($\pi N \rightarrow \pi N$: GW-SAID WI08 (ED solution))

• $\gamma N \rightarrow X$:



New: $\pi N \rightarrow \omega N$ [Yu-Fei Wang 2022]

New: Updated fit (C. Schneider talk at 10:15 am)

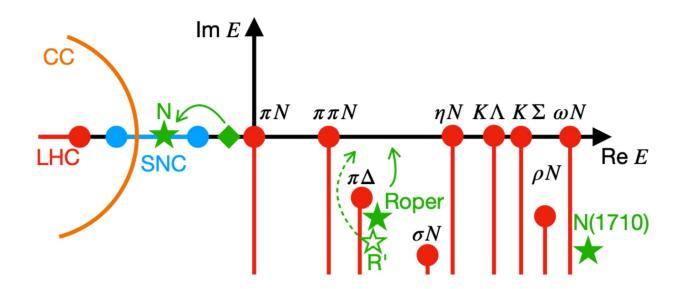
Reaction	Observables (# data points)	p./channel
$\gamma p o \pi^0 p$	$d\sigma/d\Omega$ (18721), Σ (2927), P (768), T (1404), $\Delta\sigma_{31}$ (140),	
	G (393), H (225), E (467), F (397), $C_{x'_{L}}$ (74), $C_{z'_{L}}$ (26)	25,542
$\gamma p o \pi^+ n$	$d\sigma/d\Omega$ (5961), Σ (1456), P (265), T (718), $\Delta\sigma_{31}$ (231),	
	G (86), H (128), E (903)	9,748
$\gamma p o \eta p$	$d\sigma/d\Omega$ (9112), Σ (403), P (7), T (144), F (144), E (129)	9,939
$\gamma p o K^+ \Lambda$	$d\sigma/d\Omega$ (2478), P (1612), Σ (459), T (383),	
	$C_{x'}$ (121), $C_{z'}$ (123), $O_{x'}$ (66), $O_{z'}$ (66), O_x (314), O_z (314),	5,936
$\gamma p o K^+ \Sigma^0$	$d\sigma/d\Omega$ (4271), P (422), Σ (280), T (127), $C_{x',z'}$ (188), $O_{x,z}$ (254)	5,542
$\gamma p o K^0 \Sigma^+$	$d\sigma/d\Omega$ (242), P (78)	320
	in total	57,027

New interface [https://jbw.phys.gwu.edu/]



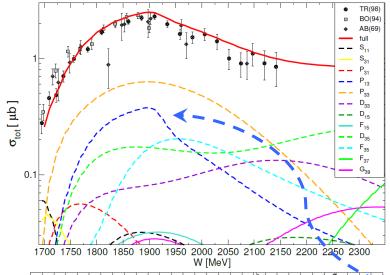
Partial-Wave Analytic structure

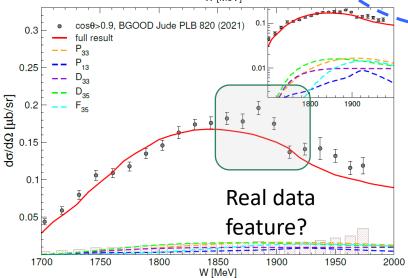
- Branch points indicate thresholds
- Partial-wave amplitudes have more cuts than plane-wave amplitude
- Example: The structure of the P11 amplitude



Resonances in $K\Sigma$ photoproduction

$$\gamma p \to K^+ \Sigma^0$$





Similarly: $K^0\Sigma^+$

[D. Roenchen et al. (EPJA 2022)]

[Webpage all results]

dominant partial waves: I = 3/2

Exception: P_{13} partial wave (I = 1/2):

N(1720) 3/2 ⁺	Re E_0	$-2 \text{Im } E_0$	$\frac{\Gamma_{\pi N}^{1/2} \Gamma_{K\Sigma}^{1/2}}{\Gamma_{\text{tot}}}$	$\theta_{\pi N \to K\Sigma}$
* * **	[MeV]	[MeV]	[%]	[deg]
2022	1726	185	5.9	82
2017	1689(4)	191 (3)	0.6(0.4)	26(58)
PDG 2021	1675 ± 15	250^{+150}_{-100}	_	_

 N(1900) 3/2 ⁺	Re E_0	$-2 \text{Im } E_0$	$\frac{\Gamma_{\pi N}^{1/2} \Gamma_{K\Sigma}^{1/2}}{\Gamma_{\text{tot}}}$	$\theta_{\pi N \to K\Sigma}$
* * **	[MeV]	[MeV]	[%]	[deg]
2022	1905	93	1.3	-40
2017	1923 (2)	217 (23)	10(7)	-34(74)
PDG 2021	1920±20	150 ± 50	4±2	110±30

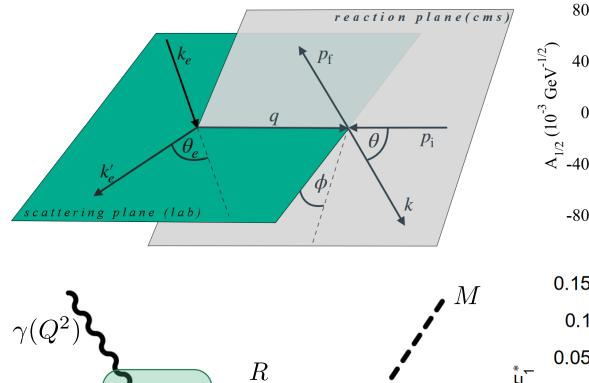
drop in cross section ("cusp-like structure") due to $N(1900)3/2^+$

N(1535) ½-	Re E_0	$-2 \text{Im } E_0$
* * **	[MeV]	[MeV]
2022	1504(0)	74 (1)
2017	1495(2)	112(1)
PDG 2021	1510 ± 10	130 ± 20

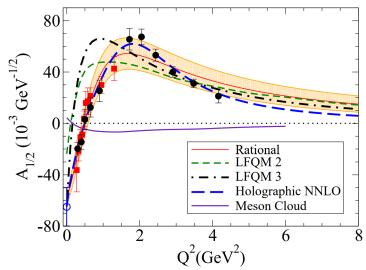
New, wide dynamically generated states in $J^P=3/2^{-1}$

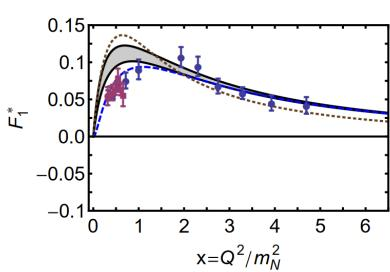


Electroproduction reveals resonance structure









Proton-Roper Transition [Burkert] [Segovia]

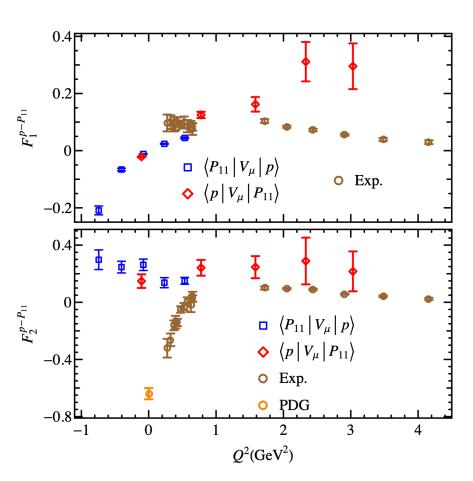


Baryon TFFs from Lattice

Meson sector: See J. Dudek talk Tuesday

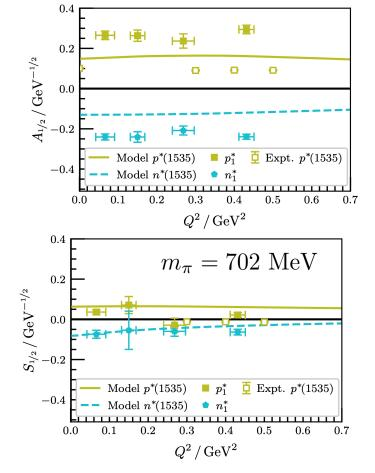
Proton-Roper

[<u>H.-W. Lin et al.</u> (2008)]



• N(1535)1/2-

[<u>F.-M. Stokes et al.</u> (2024)]





Electroproduction Analysis efforts

- **MAID**: electroproduction of pions, eta mesons, and kaons in separate approaches [<u>Tiator 2007</u>]
- **JM (JLab)** approach: single-pion analysis, double pion analysis [Mokeev, PRC 2023]
- ANL-Osaka: Single-pion electroproduction, using multi-channel model. [Kamano, Lee, Nakamura, Sato, 2016]
- **JBW**: simultaneous analysis of multiple electroproduction final states, using multi-channel model







M. Mai

Yu-Fei Wang

Coupled-Channel Electroproduction

First coupled-channel electroproduction analysis of different final states

(2020 -)

Formalism

- Photoproduction solution as constraint
- Constraints from (Pseudo)-threshold:

$$(E_{l+}^I, L_{l+}^I) \to k^l q^l \quad (l \ge 0)$$

$$(M_{l+}^I, M_{l-}^I) \to k^l q^l \quad (l \ge 1)$$

$$(L_l^I) \to kq \quad (l = 1)$$

$$(E_{l-}^I, L_{l-}^I) \to k^{l-2} q^l (l \ge 2)$$

Siegert's theorem

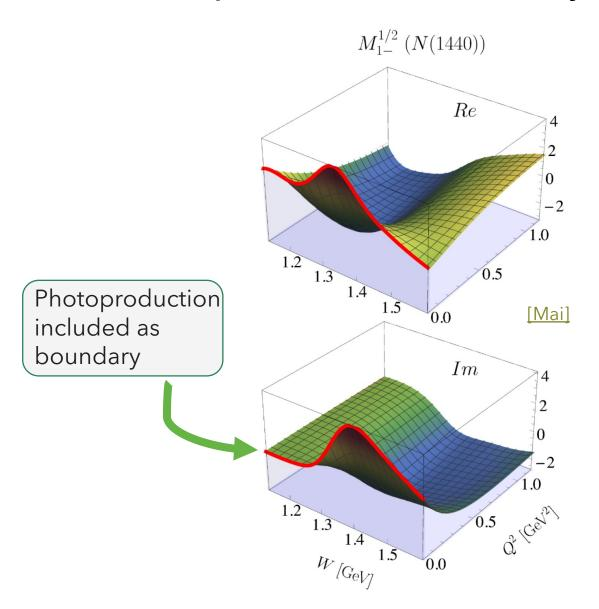
$$rac{E_{l_+}}{L_{l_+}}
ightarrow 1, \qquad \qquad rac{E_{l_-}}{L_{l_-}}
ightarrow rac{-l}{l-1}$$
 at pseudo-threshold

Amaldi, Fubini, Furlan, Springer Tracts Mod. Phys. 83, 1 (1979) Tiator, Few-body Systems 57, 1087 (2016)

Watson's theorem, multi-channel unitarity

$$\begin{split} M_{\mu\gamma^*}(q,W,Q^2) &= V_{\mu\gamma^*}(q,W,Q^2) + \sum_{\kappa} \int dp p^2 T_{\mu\kappa}(q,p,W) G_{\kappa}(p,W) V_{\nu\gamma^*}(p,W,Q^2) \\ V_{\mu\gamma^*}(p,W,Q^2) &= \alpha_{\mu\gamma^*}^{NP}(p,W,Q^2) + \sum_{i} \frac{\gamma_{\mu;i}^a(p) \gamma_{\gamma^*;i}^c(W,Q^2)}{W - m_i^b} \end{split} \quad \begin{array}{l} \text{Resonances, background, channels have independent } \\ Q^2 \text{ dependence for flexible} \end{split}$$

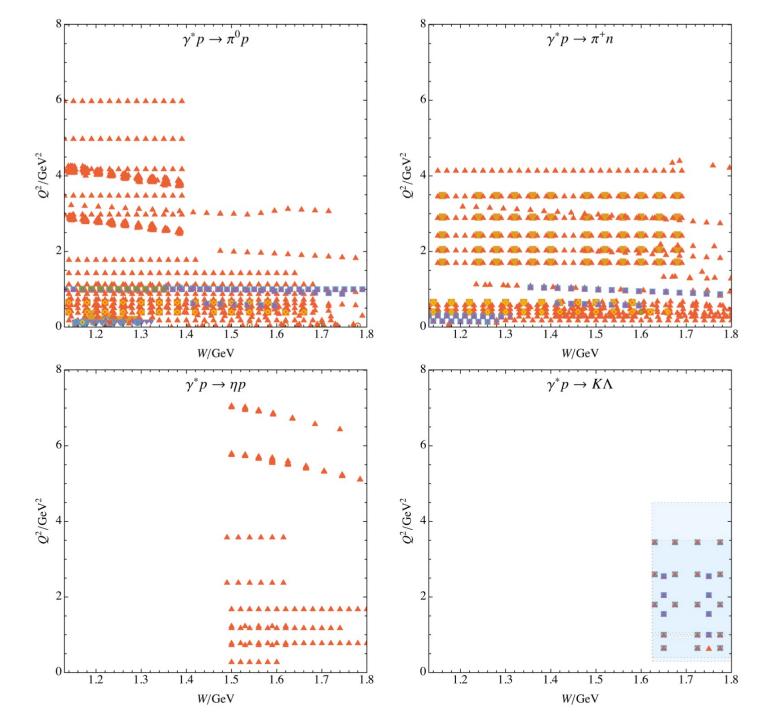
Photoproduction boundary



JBW Electroproduction data base

Type	$N_{ m data}^{\pi^0 p}$	$N_{ m data}^{\pi^+ n}$	$N_{ m data}^{\eta p}$	$N_{ m data}^{K\Lambda}$
$ ho_{LT}$	45	_	_	_
$ ight ight ho_{LT'}$	2768	5068	_	_
$lack \sigma_L$	_	2	_	_
$\wedge d\sigma/d\Omega$	48135	44266	3665	2055
$\nabla \sigma_T + \epsilon \sigma_L$	384	182	_	204
\circ σ_T	30	2	_	_
\square σ_{LT}	373	138	_	204
$\diamond \sigma_{LT'}$	214	208	_	156
$\triangle \sigma_{TT}$	327	123	_	204
∇K_{D1}	1527	_	_	_
• P _Y	_	2	_	_
Total	53804	49989	3665	2823

- Data base grown over decades with recent input mostly by CLAS, MAMI.
- Far from complete: Kinematic gaps & consistency issues. Need to combine information from different (W, Q^2) regions
- Need to combine information from simultaneous analysis of different final states ($\pi N/\eta N/KY/\pi \pi N,...$) to extract resonance helicity couplings





Fit details: Weighted vs. unweighted χ^2

- Meson production data bases are heterogeneous:
 - A few polarization measurements with large error bars (small weight in χ^2)
 - Many cross section data with smaller error bars (large weight in χ^2)
 - ... but those **few** polarization possess **great** power to discriminate solutions
- Introduce **weighted** vs.

unweighted χ^2 :

$$\chi_{\text{wt}}^2 = \sum_{j \in \{\pi^0 p, \pi^+ n, \eta p\}} \frac{N_{\text{all}}}{3N_j} \sum_{i=1}^{N_j} \left(\frac{\mathcal{O}_{ji}^{\text{exp}} - \mathcal{O}_{ji}}{\Delta_{ji}^{\text{stat}} + \Delta_{ji}^{\text{syst}}} \right)^2. \qquad \qquad \chi_{\text{reg}}^2 = \sum_{i=1}^{N_{\text{all}}} \left(\frac{\mathcal{O}_{i}^{\text{exp}} - \mathcal{O}_{i}}{\Delta_{i}^{\text{stat}} + \Delta_{i}^{\text{syst}}} \right)^2$$

Quote results for both cases



Fit Strategies (πN)

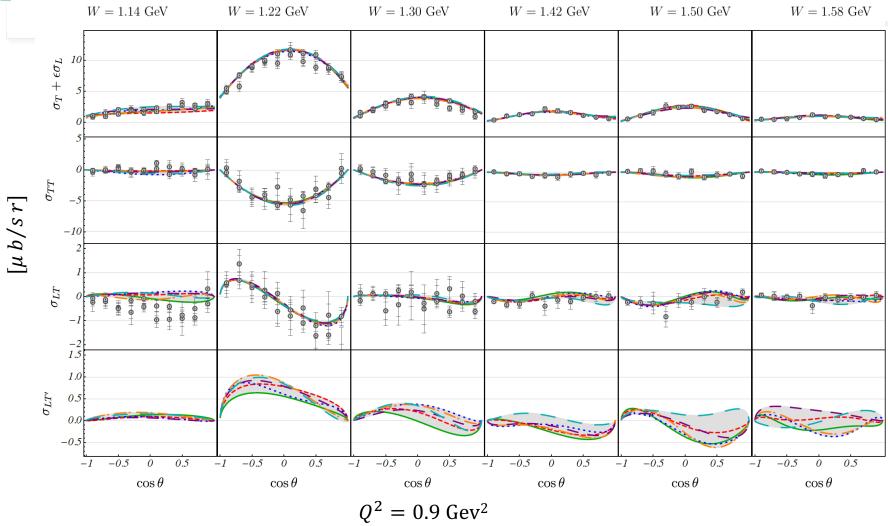
[M. Mai et al, 2021]

- Different fit strategies for $N \approx 85,000$ data in $\gamma^* N \to \pi N, \eta N$:
 - Sequential S → S+P → S+P+D waves;
 - Subsets of data until full data set reached
 - Simultaneous fit all parameters (209) set to zero without any (!) guidance
 - Extend data range from $0 < Q^2 < 4~{\rm Gev^2}$ to $0 < Q^2 < 6~{\rm Gev^2}$ to check for stability

Fit	(σ_L	$d\sigma_{j}$	$/d\Omega$	$\sigma_T +$	$-\epsilon\sigma_L$	σ	σ_T	σ_{I}	LT	σ_{I}	LT'	σ_{T}	r_T	K_{1}	D1	I	\mathcal{O}_{Y}	ρ_{I}	LT	ρ_{I}	LT'	$\chi^2_{ m dof}$
FIL		$\pi^+ n$	$\pi^0 p$	$\pi^+ n$	$\pi^0 p$	$\pi^+ n$	$\pi^0 p$	$\pi^+ n$	$\pi^0 p$	$\pi^+ n$	$\pi^0 p$	$\pi^+ n$	$\pi^0 p$	$\pi^+ n$	$\pi^0 p$	$\pi^+ n$	$\pi^0 p$	$\pi^+ n$	$\pi^0 p$	$\pi^+ n$	$\pi^0 p$	$\pi^+ n$	$\chi_{ m dof}$
\mathfrak{F}_1	_	9	65355	53229	870	418	87	88	1212	133	862	762	4400	251	4493	_	234	_	525	_	3300	10294	1.77
\mathfrak{F}_2	_	4	69472	55889	1081	619	65	78	1780	150	1225	822	4274	237	4518	_	325	_	590	_	3545	10629	1.69
\mathfrak{F}_3	_	8	66981	54979	568	388	84	95	1863	181	1201	437	3934	339	4296	_	686	_	687	_	3556	9377	1.81
\mathfrak{F}_4	_	22	63113	52616	562	378	153	107	1270	146	1198	1015	4385	218	5929	_	699	_	604	_	3548	11028	1.78
\mathfrak{F}_5	_	20	65724	53340	536	528	125	81	1507	219	1075	756	4134	230	5236	_	692	_	554	_	3580	11254	1.81
F 6	_	18	71982	58434	1075	501	29	68	1353	135	1600	1810	3935	291	5364		421	-	587		3932	11475	1.78



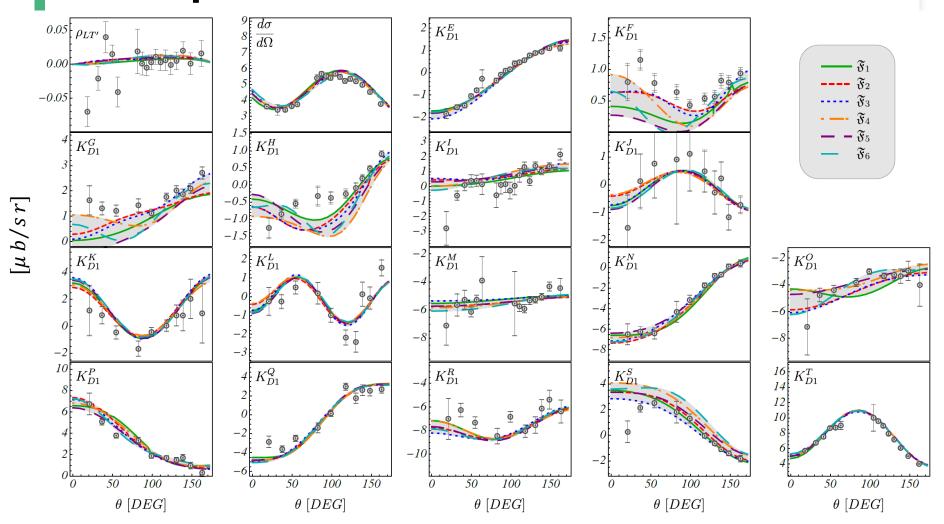
Structure functions $\pi^0 p$ (not fitted)



Data: CLAS, Phys. Rev. C (2003) <u>0301012 [nucl-ex]</u>, Phys. Rev. Lett. (2002) <u>0110007 [hep-ex]</u>



Description of Polarization Observables (πN)

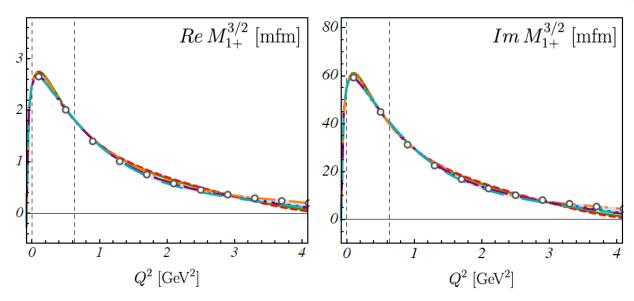


 $\pi^0 p$, Q²=1 GeV², W=1.23 GeV, ϕ =15⁰

J. J. Kelly, <u>Phys. Rev. Lett. 95 (2005)</u>.

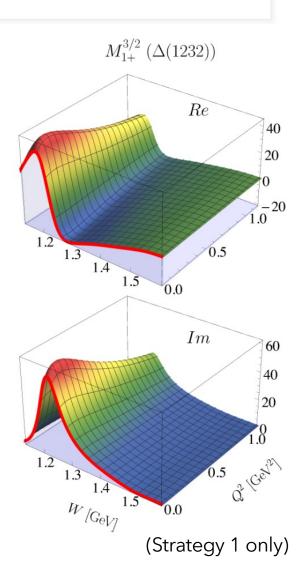


Large Multipoles



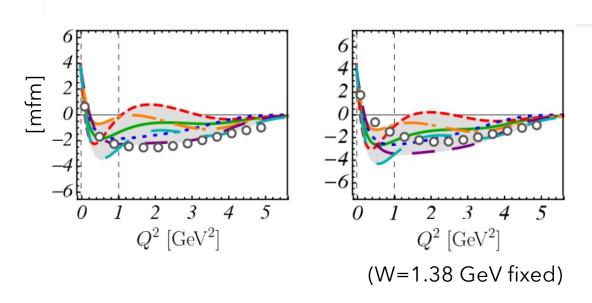
Fit strategies 1-6 together with MAID (open dots) for the magnetic multipole of the $\Delta(1232)$ Drechsel et al., EPJA (2007) 0710.0306 [nucl-th]

Prominent multipoles are well determined

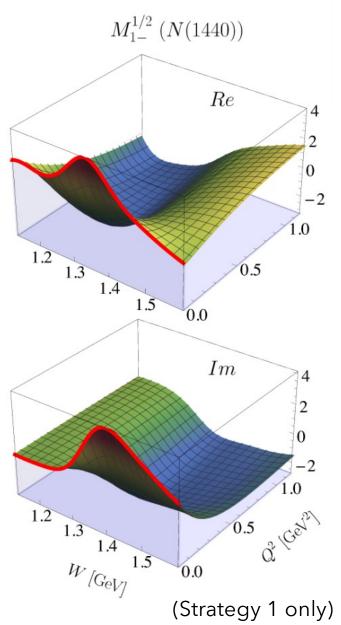




Roper Multipole



- Zero-transition (agrees with MAID)
- Extensive exploration of parameter space reveals ambiguities in PWA and reflects systematic uncertainties

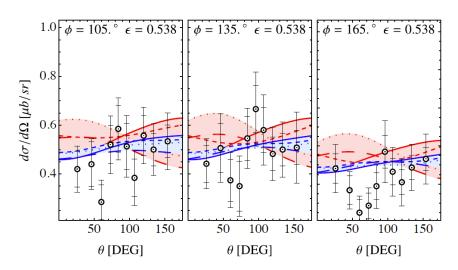


η Electroproduction

[M. Mai et al., PRC (2022)]

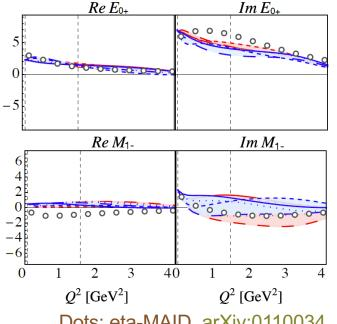
- $N_{data}^{\eta p} = 1,874$ (only $d\sigma/d\Omega$) (84,842 in total)
- kinematic range: $0 < O^2 < 4 \text{ GeV}^2$, 1.13 < W < 1.6 GeV
- 8 different fit strategies: 4 with standard χ^2 , 4 with weighted χ^2 to account for the smaller $N_{data}^{\eta p}$ \rightarrow better data description with weighted fit strategies:

Selected fit results: $\gamma^* p \to \eta p$ at W = 1.5 GeV, $Q^2 = 1.2 \,\text{GeV}^2$. Data: Denizli et al. (CLAS) PRC 76 (2007)



Upcoming: Polarization observables! Talk **Izzy Illari**

Selected multipoles at W = 1535 MeV



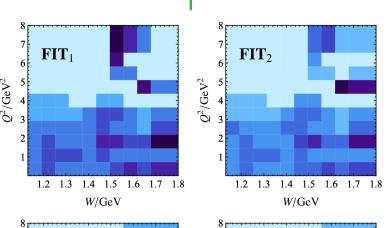
Dots: eta-MAID, arXiv:0110034

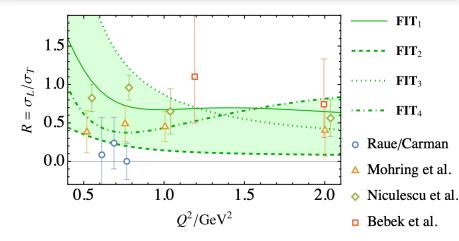


Kaon electroproduction

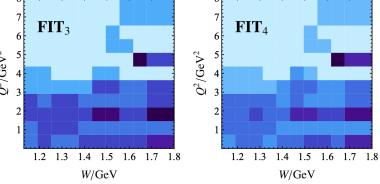
[M. Mai et al., EPJA 2023]

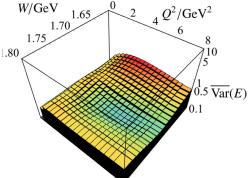
	$\chi^2_{ m dof}$	$\left \chi^2_{ m pp}(\pi^0 p) ight $	$\chi^2_{ m pp}(\pi^+ n)$	$\chi^2_{ m pp}(\eta p)$	$\left(\chi^2_{ m pp}(K^+\Lambda) ight)$
$\overline{\mathbf{FIT}_1}$	1.42	1.40	1.47	1.49	0.70
\mathbf{FIT}_2	1.35	1.38	1.35	1.40	0.58
	$\chi^2_{ m wt,dof}$	$\chi^2_{ m pp}(\pi^0 p)$	$\chi^2_{ m pp}(\pi^+ n)$	$\chi^2_{ m pp}(\eta p)$	$\chi^2_{ m pp}(K^+\Lambda)$
$\overline{\mathbf{FIT}_3}$	1.12	1.44	1.61	1.08	0.33
\mathbf{FIT}_4	1.06	1.42	1.44	1.09	(0.32)

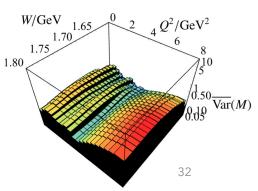




$$\overline{\operatorname{Var}}(W, Q^2)(X) := \sum_{\ell \pm} \frac{\operatorname{Var}\{|X_{\ell \pm, i}|\}}{\operatorname{Mean}\{|X_{\ell \pm, i}|\} + \varepsilon}$$





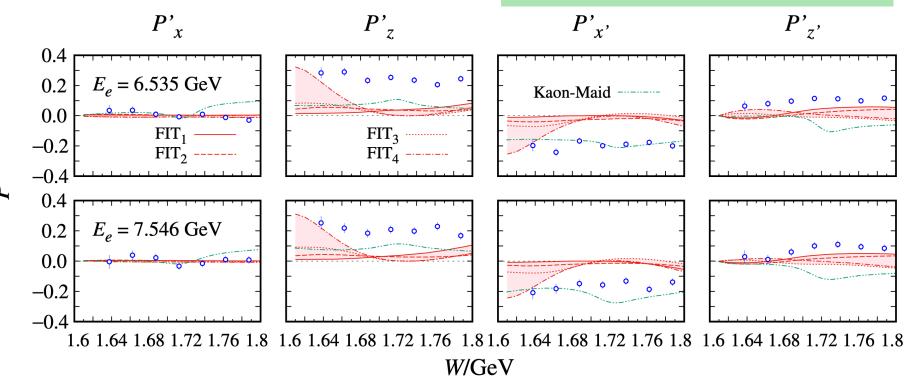




K A Challenges: Polarization measurements

- During analysis, first polarization data became available by CLAS:
- Predicted, not fitted

Beam-recoil polarization transfer [Carman et al. 2022]

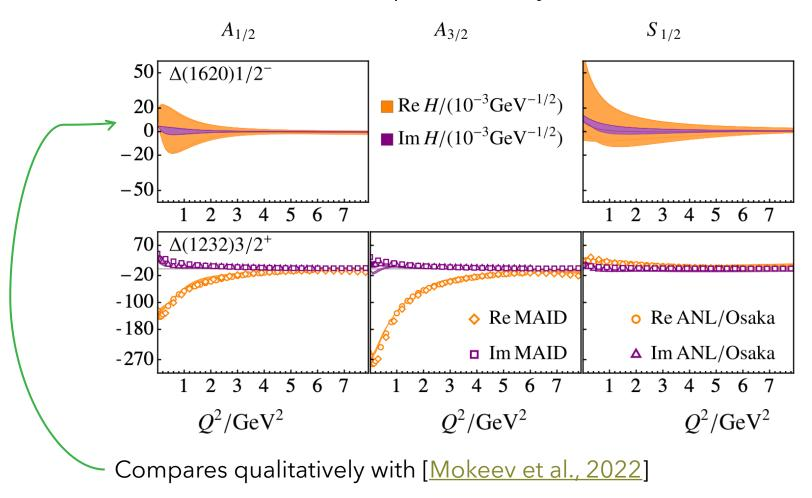




Helicity Couplings I

[<u>Yu-Fei Wang et al., 2024</u>]

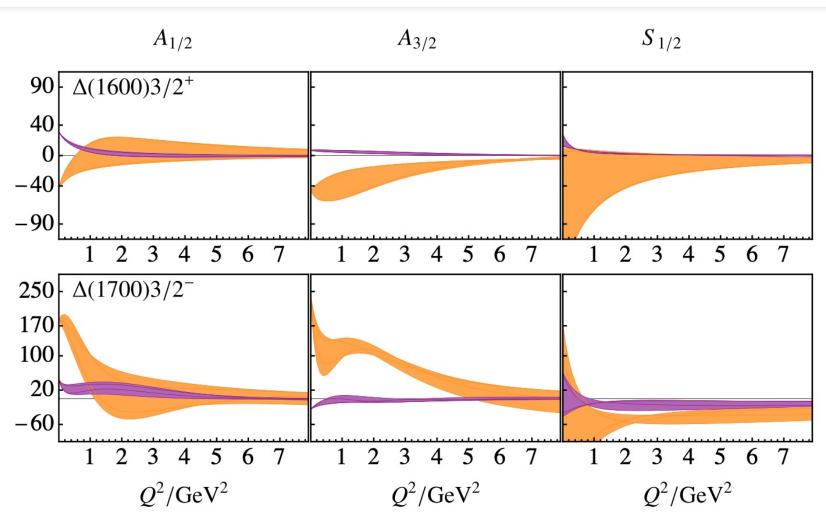
Determined at resonance poles/ many for the first time





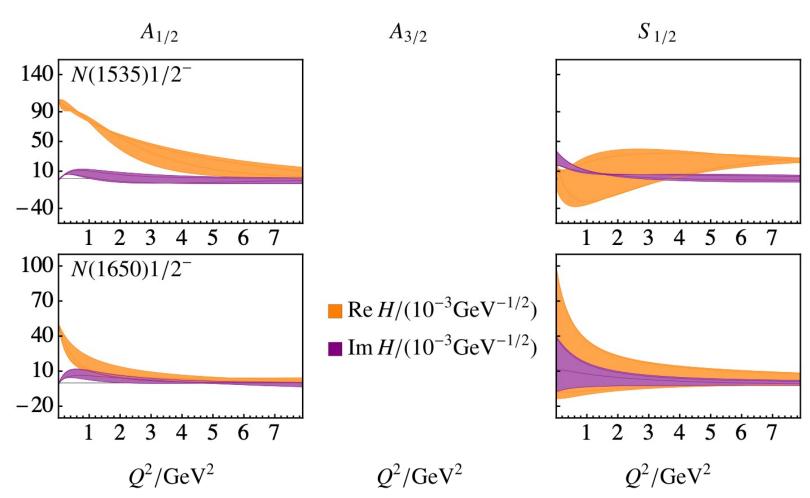
Helicity Couplings II

[Yu-Fei Wang et al., 2024]





Helicity Couplings III



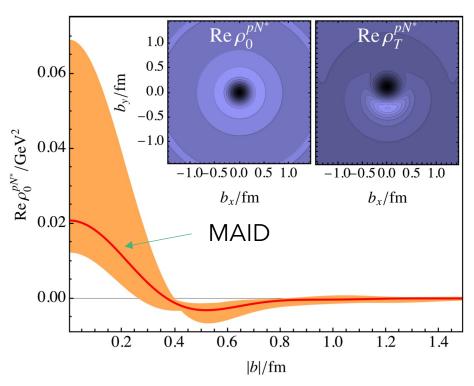


Results for the Roper resonance

Charge density structure

[approx./ following Tiator et al., (2009)]

$$\begin{split} \rho_0^{NN^*}(\vec{b}) & \equiv \int \frac{d^2\vec{q}_\perp}{(2\pi)^2} \, e^{-i\,\vec{q}_\perp \cdot \vec{b}} \, \frac{1}{2P^+} \times \\ & \langle P^+, \frac{\vec{q}_\perp}{2}, \lambda \, | \, J^+(0) \, | \, P^+, -\frac{\vec{q}_\perp}{2}, \lambda \rangle, \end{split}$$



Machine learning for partial-wave analysis

Exciting new developments: **Deep learning/neural networks** for

- Coupled-channel scattering [Sombillo, Ikeda, Sato, Hosaka, 2021]
- Resonance poles [Sombillo, Ikeda, Sato, Hosaka, 2022]
- Threshold structures [Sombillo, Ikeda, Sato, Hosaka, 2021]
- Near-threshold structures [Jpac, 2021]

Model selection for baryon analysis:

- How many partial waves are needed to describe a given data set?
 Phys.Rev.C 95 (2017) 1, 015203
- How many resonance are needed to describe a given data set?
 Phys.Rev.D 99 (2019) 1, 016001



Summary

- Juelich-Bonn-Washington/JBW model: Phenomenology of excited baryons through coupled-channels, two- and three-body dynamics.
- Renewed effort to explore additional reaction channels in the last years:

```
• \gamma p \to K \Sigma

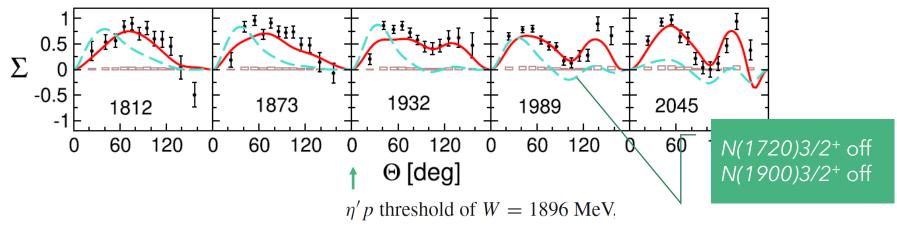
• \pi N \to \omega N

• \gamma^* p \to \pi N, \eta N, K \Lambda (Electroproduction)
```

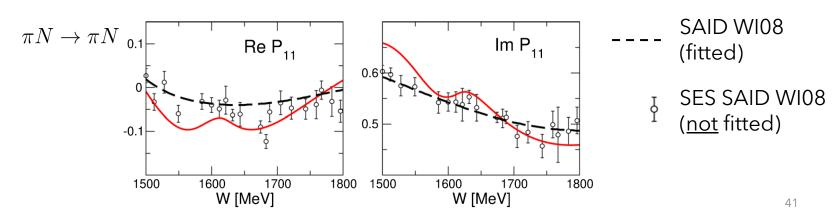
- First global electroproduction analysis of different final states
- "Extensive" exploration of parameter space with good χ^2 (better than MAID) leads to *significant* variance of some multipoles.
- Many transition form factors at the pole extracted for the first time.
- Open questions:
 - How to get solid statistical statements out of a heterogeneous data base dominated by systematic errors?
 - Blinding spectroscopy

2022 Update in other reactions

• Beam asymmetry in η photoproduction (different W)



• N(1710)1/2+ returns with large η N and K Λ branching ratios



Parametrization - Details

Dependence on virtuality: Channel and resonance-wise:

$$\tilde{F}_{\mu}(Q^{2}) = \tilde{F}_{D}(Q^{2}) e^{-\beta_{\mu}^{0} Q^{2}/m^{2}} P^{N}(Q^{2}/m^{2}, \vec{\beta}_{\mu})$$

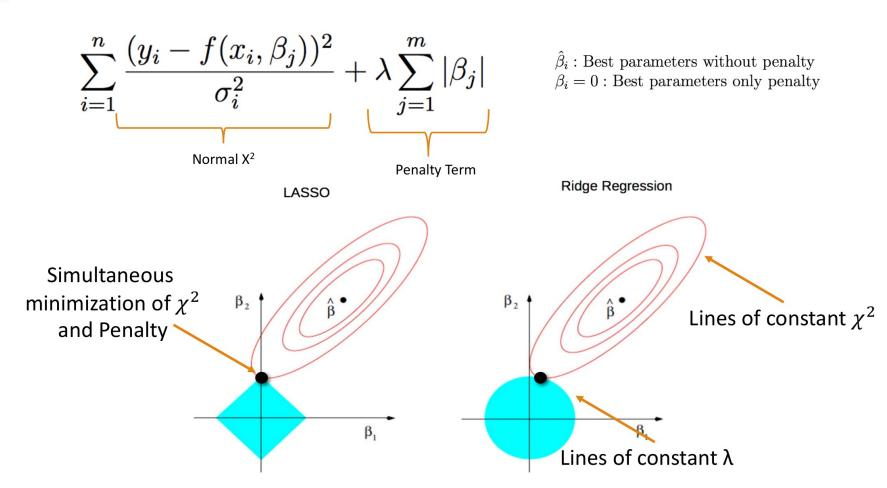
$$\tilde{F}_{i}(Q^{2}) = \tilde{F}_{D}(Q^{2}) e^{-\delta_{i}^{0} Q^{2}/m^{2}} P^{N}(Q^{2}/m^{2}, \vec{\delta}_{i})$$

Factorization:

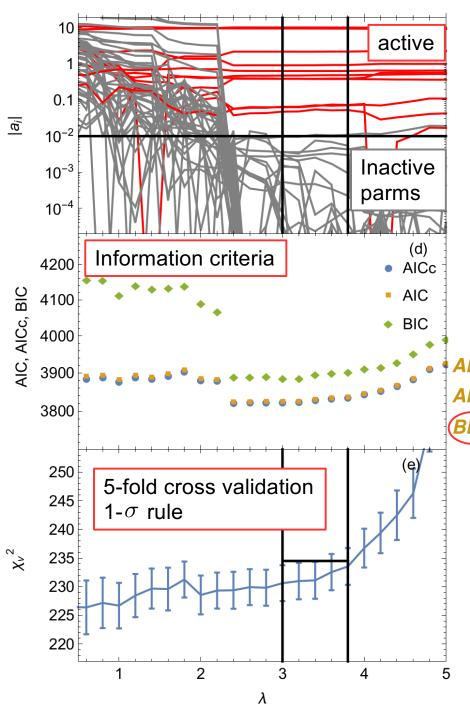
$$\alpha_{\mu\gamma^*}^{NP}(p, W, Q^2) = \tilde{F}_{\mu}(Q^2)\alpha_{\mu\gamma}^{NP}(p, W)$$
$$\gamma_{\gamma^*;i}^c(W, Q^2) = \tilde{F}_i(Q^2)\gamma_{\gamma;i}^c(W)$$

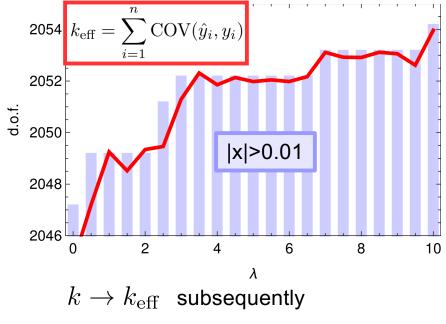


Least Absolute Shrinkage and Selection Operator (LASSO)



See, e.g.: *The Elements of Statistical Learning*: Data Mining, Inference, and Prediction, T. Hastie, R. Tibshirani, J. Friedman, Springer 2009 second ed.





$$AIC = -2 \max \log(L(\hat{\theta}|data)) + 2k = \chi^2 + 2k$$

$$AIC_c = AIC + \frac{2k(k+1)}{n-k-1}$$

$$BIC = -2 \max \log(L(\hat{\theta}|data)) + 2\log(n) = \chi^2 + k \log(n)$$

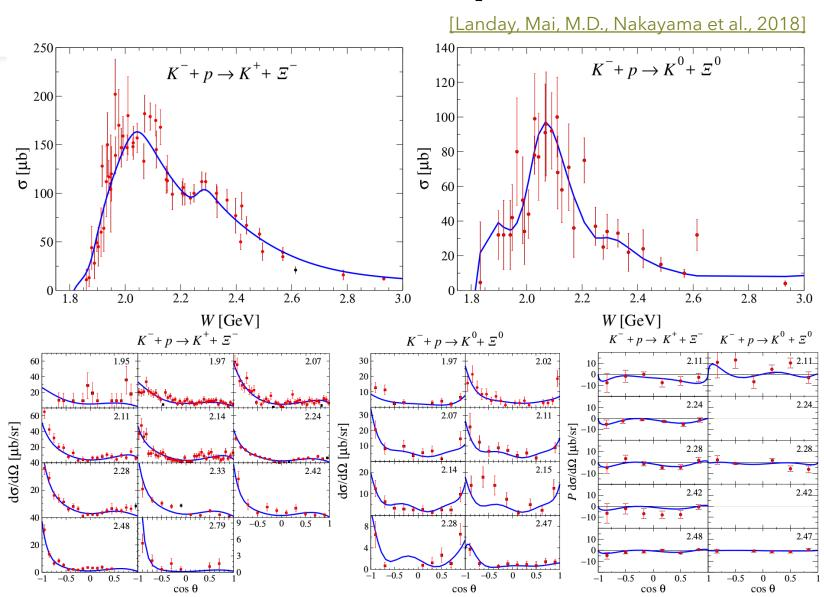
Close relation to <u>Bayesian model comparison</u> (here: $n \gg k$)

Determine the simplest model:

- Cross validation
- Information criteria

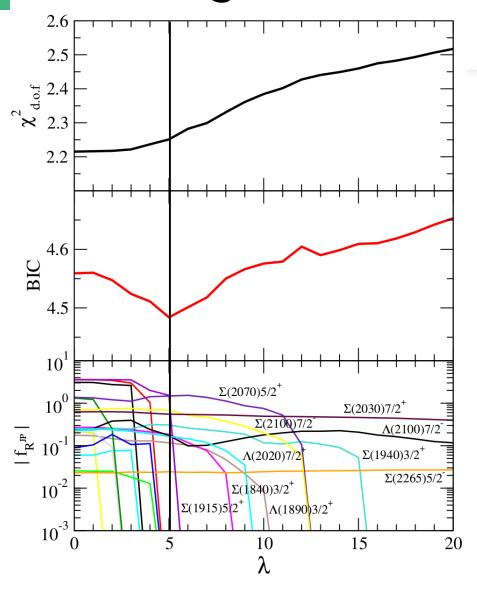


LASSO for the reaction $K^-p \to K\Xi$





LASSO regularization



[Landay, Mai, M.D., Nakayama et al., 2018]

- Self-consistent data pruning for outliers using smoothness as criterion (10 out of 448 removed)
- All 21 resonance candidates from PDG
- Masses and widths fixed to PDG values
- Only Couping constants fitted
- 10 out of 21 resonances automatically selected by LASSO.

See also J. Oh's talk on this conference on Cascade production